Renewable Energy xxx (xxxx) 1–14

Contents lists available at ScienceDirect

Renewable Energy

journal homepage: www.elsevier.com/locate/renene

Experimental thermal performance evaluation of different configurations of Copenhagen solar cooker

Xabier Apaolaza-Pagoaga [a, *], Antonio Carrillo-Andrés [a], Celestino Rodrigues Ruivo [b, c]

[a] Energy Research Group. Department of Mechanical, Thermal and Fluids Engineering, University of Malaga. Calle Arquitecto Francisco Peñalosa, 6, 29071, Malaga, Spain
[b] Department of Mechanical Engineering, Institute of Engineering, University of Algarve, Campus da Penha, 8005-139 Faro, Portugal
[c] ADAI - LAETA, Rua Pedro Hispano nº12, 3030-289, Coimbra, Portugal

ARTICLE INFO

Article history:
Received 28 June 2021
Received in revised form 9 October 2021
Accepted 27 November 2021

Keywords:
Solar cooking
Copenhagen cooker
Experimental test
Solar energy

ABSTRACT

In this work, four different configurations of Copenhagen solar cookers were tested experimentally at the same time under the same weather conditions. First tests were carried out using pots without water load. Secondly, tests were performed with the equal amount of water in each pot. Thirdly, tests were carried out with different amounts of water for one of the configurations. From the results of the first set of tests, it was found that the performance of one of the configurations depends more significantly on the solar altitude angle than the others. A large number of experiments for each set of tests were conducted covering a wide range of solar altitude angles. A thermal performance analysis based on the ASAE S580.1 standard was performed with the measured data of the second and third sets of tests. The obtained plots with the observation points of each configuration evidence that the linear trend of the standardised power is not universal. The observed trends are very dependent on the solar altitude angle. Thus, the procedure for evaluating standardised power recommended by the standard for cooker performance comparison should be improved.

Nomenclature

$A_{n,max}$	Maximum normal area to the incoming beam irradiation being collected by the solar cooker (m^2)
a	Slope of the linear regression of standardised power (W °C^{-1})
c_w	Specific heat of water (J kg^{-1}°C)
I	Solar irradiance (W m^{-2})
I_{bn}	Beam normal solar irradiance (W m^{-2})
$\bar{I}_{bn}$	Average beam normal solar irradiance during a test (W m^{-2})
I_n	Global normal solar irradiance (W m^{-2})
$\bar{I}_n$	Average global normal solar irradiance during a test (W m^{-2})
m_w	Mass of water (kg)
n_p	Number of valid observation points for deriving the linear regression
n_t	Number of tests
$\dot{Q}$	Cooker power (W)
$\dot{Q}_S$	Standardised cooker power (W)
$\dot{Q}_{S,0}$	Standardised cooker power for $\Delta T_{w,a} = 0$°C (W)
$\dot{Q}_{S,50}$	Standardised cooker power for $\Delta T_{w,a} = 50$°C (W)
$\dot{Q}_{S,CI\ 95\%}$	95% confidence interval for the standardised power (W)
$\dot{Q}_{S,PI\ 95\%}$	95% prediction interval for the standardised power (W)
R^2	Coefficient of determination (–)
T_a	Outside air temperature (°C)
$T_{a,pot}$	Air temperature inside the pot in experiments without water load (°C)
$\bar{T}_a$	Average ambient temperature during a test (°C)
T_w	Load temperature (°C)
v_a	Wind velocity (m s^{-1})
$\bar{v}_a$	Average wind velocity during a test (m s^{-1})

Greek symbols

α_s	Solar altitude angle (º)
$\bar{\alpha}_s$	Average solar altitude angle during a test (º)
η_{50}	Thermal conversion efficiency for $\Delta T_{w,a} = 50$ °C
$\Delta\dot{Q}_S$	Residual standardised power (W)
Δt_i	Time interval (s)

https://doi.org/10.1016/j.renene.2021.11.105
0960-1481/

$\Delta T_{w,i}$ Increase of water temperature for each time interval (ºC)
$\Delta T_{w,a}$ Difference between water load and ambient temperature (ºC)

Subscripts

n Direction normal to beam radiation
i Time interval *i*

Abbreviations

CC*j* Solar cooker number *j*

1. Introduction

The use of solar cookers has several advantages. Solar energy is free and widely available in many regions of the world and their use directly for solar cooking does not generate pollution. These advantages should make solar cookers interesting for many people around the world, mainly in areas where people are facing difficulties in accessing gas or electricity due to poverty or living in remote areas. In these contexts, it is important to point out that solar cooking is not a universal cooking solution, but it should be considered as part of the solution when combined with efficiency wood stoves or biomass cooking.

In last decades, many types of solar cookers have been developed [1–4]. They are usually classified into different groups: box cookers, parabolic cookers, panel cookers and evacuated tube cookers.

Panel cookers are usually low cost and portable products that are easy to be constructed with simple few tools. Most panel cooker designs provide successful cooking results when a black pot and a transparent enclosure are used. They have a great application in picnics and can mitigate some of the problems related with emergency situations such as those derived from natural disasters or those occurring in refugee camps [5–7].

The Copenhagen solar cooker can be considered a panel solar cooker made of four equal squared and light reflectors that occupies a small volume when packed. The reflectors can be assembled in different configurations. Some other panel cookers have been investigated and tested [8,9], but concerning Copenhagen cookers the scientific information about their performance is scarce [10,11]. Sharon and Gregg Clausson developed the Copenhagen solar cooker in 2009, naming after the UN Climate Conference that occurred in that year. The original Copenhagen was constructed from four flexible reflective place mats secured in position with simple clamps.

Some panel solar cookers were tested [8] by following the protocol of the ASAE S580.1 standard [12]. The small cooker Haines 1 and the larger cooker Haines 2 provided a standardised cooker power of 41 W and 82 W, respectively, when the difference between the load and outside air was 50 °C [8]. Both versions were tested by using a polycarbonate enclosure for making the greenhouse effect around the pot. A version of the well-known Cookit solar cooker [13], which has a collecting area to the incoming solar radiation similar to the area of the Haines 2 solar cooker, was tested and a standardised power value of 58 W was reported [8]. The experiments conducted with the StarFlower solar cooker, which is a deep parabolic solar cooker composed of multiple reflectors and more expensive than most common panel solar cookers, have provided a standardised power value of 117 W [8].

Ruivo et al. [9] studied the performance of a panel cooker with funnel shape by following the ASAE S580.1 standard, but they also proposed some improvements to the standard. A large number of tests were conducted by using a transparent glass lid and a metal lid on the black pot together with a massive glass enclosure to trap the heat around the pot [9]. The maximum standardised power value of 74 W was found when using the transparent lid. Ebersviller and Jetter [14] have tested a parabolic cooker, a box cooker and the panel cooker named Hotpot. The Hotpot cooker is a small size panel cooker that provided a power of only 25 W. It is equipped with a relatively big cooking vessel that was designed specifically for this cooker design.

Regattieri et al. [15] have conducted some tests of simple cookers made of cardboard and aluminium foil. The most efficient tested model was the ones composed of multiple reflectors with a maximum normal area to the incoming beam irradiation of 0.72 m^2. The authors have named this design as 'parabolic' cooker and they have estimated the overall efficiency to be in the range of 0.15–0.18.

A summary of the results of the different scientific studies is presented in Table 1.

In present work, the performances of Copenhagen solar cookers are investigated by using experimental results of testing three cookers simultaneously. Different sets of tests were conducted with different cooker configurations. The influence of the solar altitude angle on the cooker performance is firstly addressed by using results of experiments without load inside the pot. From the results of others sets of experiments with load inside the pot, the standardised power plots are determined by following the ASAE S580.1 standard. The impact of the mass of water on the standardised power is also determined for some of the configurations experimentally tested.

2. Experimental setup

The thermal performance of three commercialized Copenhagen solar cookers is investigated. Each one can be assembled to be tested in different configurations as suggested by the manufacturer. For convenience, the cookers are here called CC1, CC2 and CC3. The cookers were tested in the experimental setup of "Escuela de Ingenierías Idustriales" of the University of Malaga, Spain at latitude 36.9° N. During the experiments, azimuthal adjustments of each cooker were performed every 20 min.

Each cooker is made up of four equal square reflectors of 368 × 368 mm and a square double layer wood plate of 203 × 203 mm, that defines the cooking area where cooking pot is placed, and allows an easy assembling of the four reflectors. Each reflector is made of a self-stick reflective vinyl covering a polypropylene substrate sheet. Fig. 1 depicts the first step of assembling the four reflectors with the double wood central plate. One of the corners of each square reflector is inserted in the empty space in between the two layers of wood. All five pieces are well fixed by suitable screws. Each square reflector has white, blue and red snaps located in different positions as can be seen in Fig. 1. This helps the user in assembling the reflectors accordingly to the specific configuration to be used. The change of cooker configuration is easy and fast thanks to the snaps.

The Copenhagen solar cooker can be assembled in three different configurations, depicted in Fig. 2. As well-known, the solar altitude angle depends on the latitude, day and hour. Thus, the manufacturer recommends to choose the configuration accordingly to the solar altitude angle α_s: *i) Cave* configuration for low solar altitude angle operation ($\alpha_s < 45°$) as depicted in Fig. 2a) by joining the red snaps, *ii) Ninety* configuration for medium solar altitude angle operation ($45 < \alpha_s < 65°$) as depicted in Fig. 2b) by joining the red and blue snaps, and *iii) Flower* configuration for high solar altitude angle operation ($\alpha_s > 65°$) as depicted in Fig. 2c) by joining the white snaps.

The three configurations of the Copenhagen solar cooker have the same reflector area of 0.542 m^2, but they have different values of the maximum normal area to the incoming beam irradiation being collected by the solar cooker $A_{n,max}$: 0.174 m^2 for *Cave* configuration,

* Corresponding author.
E-mail address: apaolaza@uma.es (X. Apaolaza-Pagoaga).

Table 1
Summary of the data and results of several tested cookers.

Solar cooker model	$A_{n,max}$ (m^2)	Reflector area (m^2)	$\dot{Q}_{S,50}$ (W)	$\dot{Q}_{S,50}/A_{n,max}$ $(W\ m^{-2})$
Haines 1 [8]	0.307	0.744	41	134
CooKit [8,13]	0.467	0.848	58	124
Haines 2.0 [8]	0.500	1.210	82	164
StarFlower [8]	0.657	–	117	178
Funnel cooker [9]	0.500	1.063	74	148
Hotpot [14]	0.287	–	25	87
Regattieri [15]	0.720	–	83	115

0.238 m^2 for *Ninety* configuration and 0.197 m^2 for *Flower* configuration. These values of $A_{n,max}$ were estimated by the method developed by Arveson [16]. The largest and smallest area values are observed in *Ninety* and *Cave* configurations, respectively, being the difference of 37%. Thus, important differences in cooker performance is expected to be observed in these two configurations.

The cooking vessel here adopted is composed of a pot, a lid and a massive glass enclosure. It is centred with the square double wood plate when testing *Ninety* and *Flower* configurations and little off-centred in *Cave* configuration. The pot is made of steel with an enamel black layer. It has a diameter of 200 mm, which is close to the side length of wood plate, a maximum capacity of 3 L, a height of 100 mm, and a mass of 540 g. The glass lid of each pot has a mass of 366 g. It was used in all tests performed with water as load. A metal lid of the same material of pot with a mass of 260 g was used only in the first set of tests conducted without load to measure the temperature of the air by the thermocouples inside the pot without any direct influence of solar radiation.

The massive glass enclosure is depicted in Fig. 3. It is composed of two glass washing machine windows functioning as a greenhouse, where the pot is inserted. The mass of heat trap of cooker CC1, CC2, and CC3 are, respectively, 2250, 2207, and 2240 g.

The experimental setup used for test the three configurations of Copenhagen cooker is shown in Fig. 4. Five T-type thermocouples inside each pot, at different positions and 10 mm from the bottom of the pot, are used. The average value of the temperature of these five sensors is estimated and considered to be representative of the load temperature T_w and the air temperature $T_{a,pot}$, respectively, for the tests with and without load. These temperature values and the solar irradiance values measured by the pyranometers shown in right side of photo in Fig. 4 were logged. The weather station, shown also in right part of Fig. 4, is composed of sensors of wind speed v_a and ambient temperature T_a. The measured values also were logged. The temperature values are recorded every 15 s. Azimuthal adjustments of the two pyranometers were performed every 20 min, i.e., at the same time cookers were adjusted. One of these pyranometers was positioned horizontally and the other was placed over a tilted plane making an angle of 50° with the horizontal plane. There was a second weather station in the top of the school building in the same rooftop patio where the experiments were carried out. This station was used to measure global and diffuse solar ir-

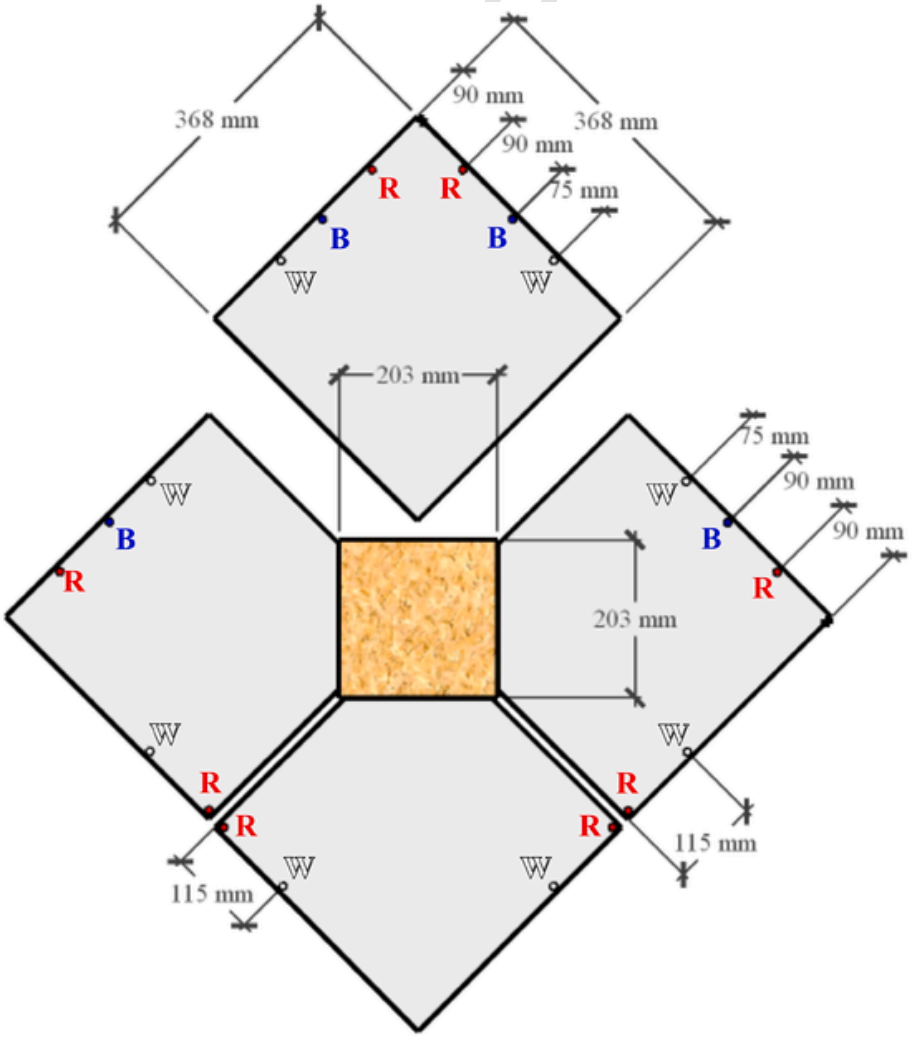

Fig. 1. First step of assembling the five pieces of a Copenhagen solar cooker.

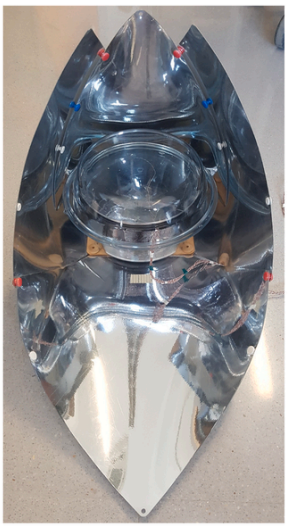

a)

b)

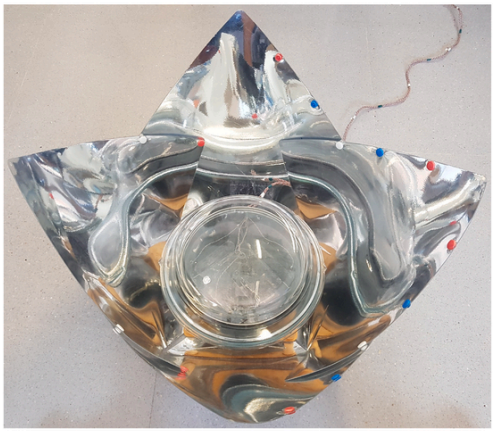

c)

Fig. 2. Configurations of the Copenhagen solar cooker: a) *Cave* b) *Ninety* and c) *Flower*.

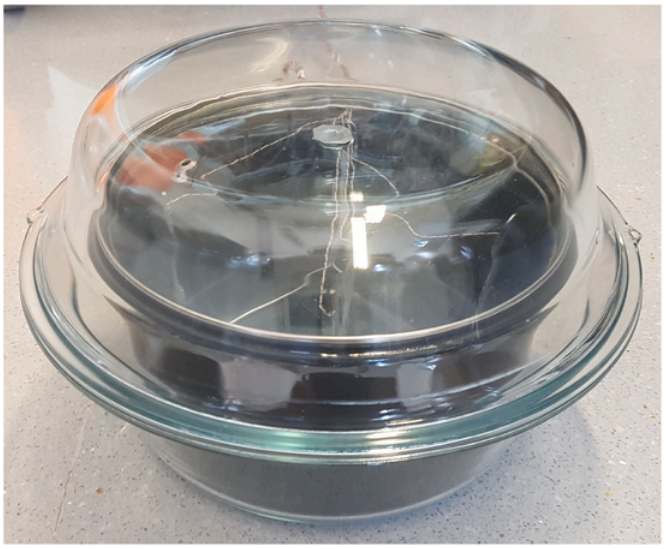

Fig. 3. Cooking set with massive glass enclosure.

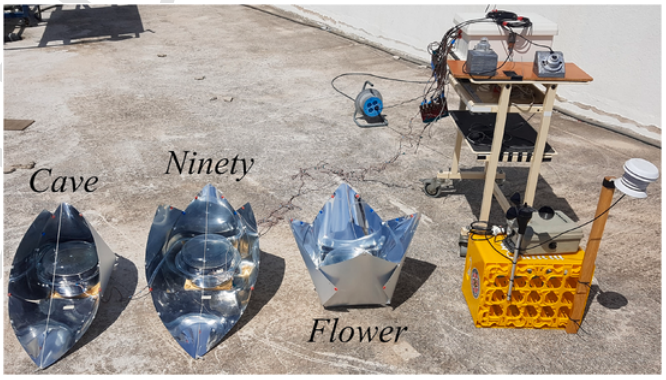

Fig. 4. Experimental setup used for testing the three cooker configurations.

radiance in the horizontal plane. Both measured variables were used to calculate the fraction of direct solar irradiance in the horizontal plane. From these measurements direct normal irradiance I_{bn} is easily calculated. However, ASAE S580.1 standard requires global normal irradiance I_n to be determined, so the Liu Jordan isotropic sky model was used for the estimation of the diffuse components of irradiance (sky and ground reflected) on a plane normal to incoming beam radiation [17]. The Liu Jordan model is simple but suitable for clear sky. Albedo was assumed to be 0.2. More of the measuring systems used in the experiments are described in Ruivo et al. [9].

3. Methods and data processing

The procedures for testing the cookers and for reporting the results here adopted are based mainly on the ASAE S580.1 standard [12]. Anyway, some of the improvements made by Ruivo et al. [9] and complementary tests to investigate the influence of the solar altitude angle on the performance of the cookers without load are also taken into account. The ASAE S580.1 standard determines the conditions under which the tests are performed [12]. It specifies the use of water as load, a ratio load of 7 kg m^{-2} and the valid ranges of the ambient temperature, wind speed and solar irradiance. Some of these constraints were not fulfilled such as the load ratio adopted in each test. In addition, in some tests, the average wind speed $\bar{v}_a$ exceeds 1 m s^{-1}, i.e., the maxi-

mum value established by the standard. As mentioned before, the different configurations have different values of $A_{n,max}$. Thus, it was decided in present work to apply the same mass of load instead of using strictly the load imposed by the standard. It is important to point out that the use of a high load ratio of 7 kg m^{-2} makes the heating up of the load too long. Moreover, it is not representative of the mass load of most solar cooked dishes in practice with this kind of panel solar cooker. For this reason, the mass load of 1.5 kg but also lower values of 1.0 kg and 0.5 kg, were adopted in present study. Table 2 shows the corresponding values of the load ratio for each cooker configuration.

For each experiment, it is important to observed how the different uncontrolled variables vary with time. It allows to verify if the ranges established by the standard were or not fulfilled. Moreover, it allows also to check if there was or not any problem with logged data. As one example, Fig. 5 shows the time evolutions of most important measured variables during the experiment no. 126A, which was carried out on 25th March 2021. The depicted variables in Fig. 5 are: *i)* the solar altitude angle α_s, the global normal solar irradiance I_n, the beam normal solar irradiance I_{bn}, *ii)* the water temperature T_w and the ambient air temperature T_a and *iii)* the average wind speed in 1 min time interval v_a. In this particular experiment, the CC1, CC2 and CC3 cookers were tested in configurations *Cave*, *Flower* and *Ninety*, respectively, under medium solar altitude angles.

Table 2
Load ratio values associated with the three tested cooker configurations.

Configuration	*Cave*	*Flower*	*Ninety*
m_w (*kg*)	Load ratio (kg m^{-2})		
0.5	2.87	2.54	2.10
1.0	5.75	5.08	4.20
1.5	8.62	7.61	6.30

The ASAE S580.1 standard [12] recommends a methodology for calculating and plotting the standardised power of a solar cooker. The technical report can be used for comparing the performance of different cooker designs. In case of the present work, it is helpful to compare the performance of the different configurations of the Copenhagen cooker. The calculation of the power is made by using measured data for several observation points, each one representing the value of time interval *i* with a duration (Δt_i) of 600 s. The power is determined by the following expression:

$$\dot{Q}_i = \frac{m_w c_w \Delta T_{w,i}}{\Delta t_i} \quad (1)$$

where m_w, c_w and $\Delta T_{w,i}$ represent, respectively, the mass, the specific heat and the temperature variation of the load. In present work, a constant value of 4180 J kg^{-1} °C^{-1} was assumed for the specific heat of water. The error of this assumption, in the range of 10–95 °C, is less than 0.3%. The standardised cooking power associated with each time interval *i* is determined by just normalizing the previous power with the reference value of global normal solar irradiance of 700 W m^{-2} by:

$$\dot{Q}_{S,i} = \dot{Q}_i \frac{700}{I_{n,i}} \quad (2)$$

where $I_{n,i}$ represents the average value of the global normal solar irradiance in the time interval *i*. By following the protocol of ASAE

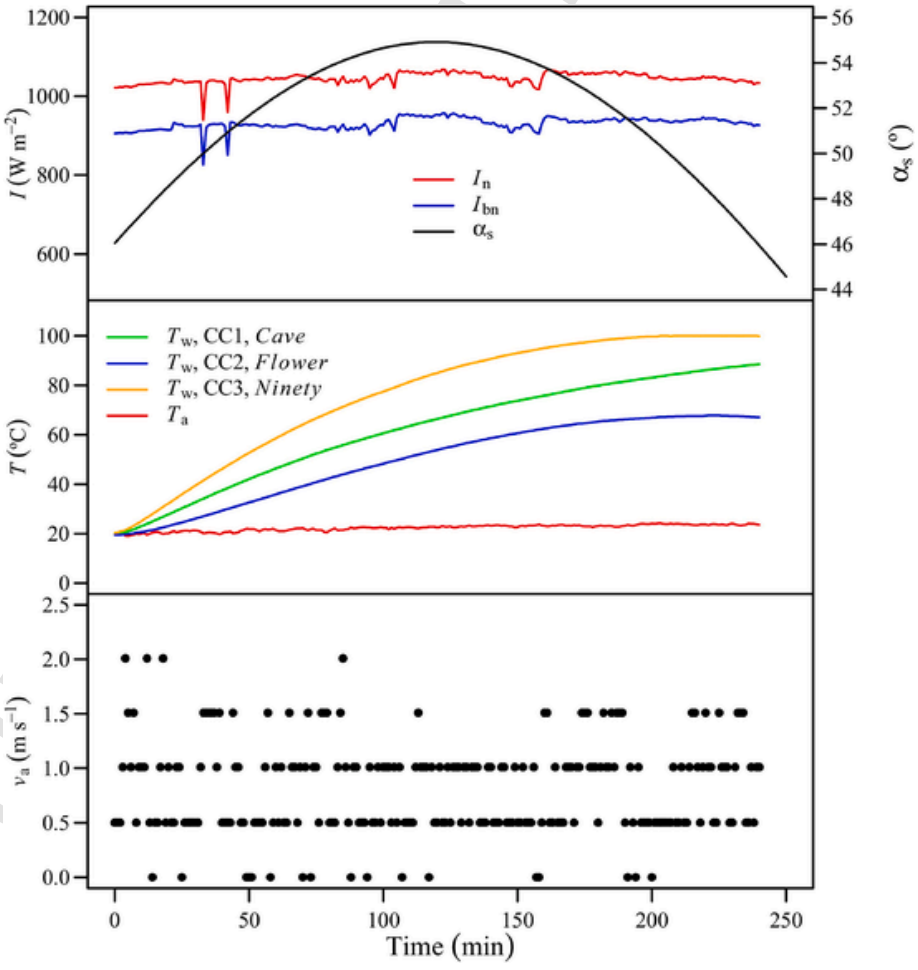

Fig. 5. Time evolutions of measured variables during the experiment no. 126A.

S580.1 standard [12], the standard cooking power $\dot{Q}_S$ values are plotted as a function of the difference between the average temperature of load and average ambient temperature, in each time interval *i*, a difference represented by $\Delta T_{w,a}$. The use of a minimum of 30 valid observation points is recommended by the standard. Thus, to fulfil this requirement, experiments must be conducted in more than one day. The standard proposes to derive the following linear regression with coefficient of determination (R^2) greater or equal to 0.75:

$$\dot{Q}_S = \dot{Q}_{S,0} + a\Delta T_{w,a} \quad (3)$$

Following the standard, the particular standardised cooking power value $\dot{Q}_{S,50}$ is calculated for a reference point where $\Delta T_{w,a}$ is equal to 50 °C.

The two statistical parameters determining the uncertainty of the linear regression, the prediction intervals $\dot{Q}_{S,PI\ 95\%}$ and the confidence intervals $\dot{Q}_{S,CI95\%}$, adopted by Ruivo et al. [9] are also considered in the analysis of the results of Copenhagen cookers.

4. Analysis of results of testing different configurations of cookers

A first set of some experiments using cookers with empty pots was performed on May 2020 and June 2020 and a large number of experiments using water as load was performed on March 2021, May 2021 and June 2021. The data of this second set of tests are listed in Table A of Appendix A.

In this section, the performance of the solar cookers without water load is firstly analysed for the different ranges of solar altitude angles. Secondly, the plots of the standardised power of the solar cooker for the different configurations and for a wide range of solar altitude angle are analysed. Thirdly, the impact of using different water mass values on the standardised power and on the time needed to heat up water to 95 °C, for a particular configuration of the cooker, is examined.

4.1. Analysis of solar cooker performance without water load

The main goal of testing the different configurations of the Copenhagen cooker without inserting water into the pot is to investigate how the solar altitude angle influences the air temperature inside the pot $T_{a,pot}$, a variable that can be seen as an important performance parameter of cooker when operating with small thermal inertia because the measured air temperature achieves much higher values, with a short delay, than the ones obtained with water. Moreover, the registered evolutions can represent also how the stagnation temperature depends on the solar altitude angle. Thus, the plots provide valuable information about what is the most suitable configuration for different ranges of solar altitude angle.

In this context, two experiments were conducted. In each experiment, the three cookers were tested side-by-side under the same uncontrolled weather variables, but assuring that, during the test period, the sky was clear, the wind speed was very low and the variation of the ambient temperature was also low.

The first experiment was performed, on 18th May 2020, by using a glass transparent lid over the pot. This cooking vessel configuration was the ones adopted in all tests made with water as load. When using a transparent lid, the extremity of each thermocouple inside the pot can be affected directly by the intense flux of incoming solar radiation concentrated in the cooking zone of the cooker. Thus, the measured value may do not represent accurately the air temperature inside the pot because the sensors do not have any shielding protection. In a second experiment, performed on 22th May 2020, an opaque lid of the same material of the pot was used in each test, actuating as a shielding device of the sensors of temperature inside the pot. The results of the tests of these two experiments are depicted in Fig. 6. The experiments were conducted between 11:00 and 16:30 solar time by making azimuthal

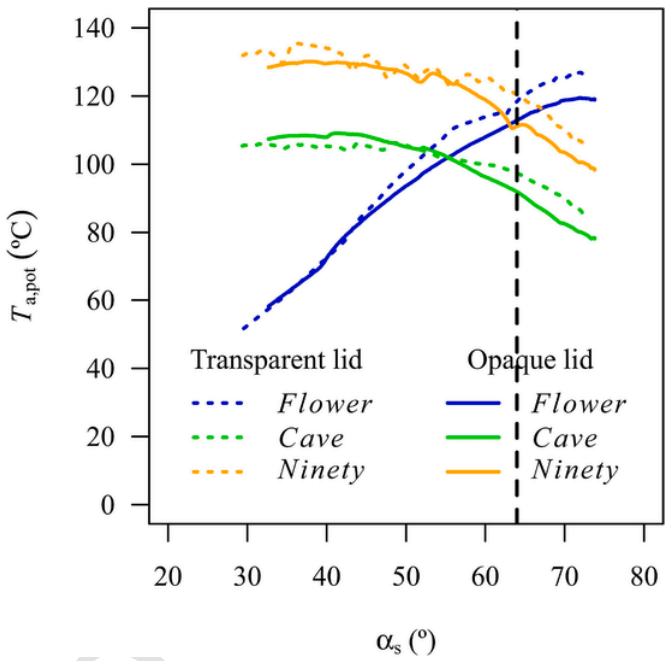

Fig. 6. Air temperature measured inside the pot for the several configurations tested.

adjustments of the cookers and of the two pyranometers every 20 min. It can be observed that the differences between the two experiments, i.e., when using the transparent lid or the metal lid, are small. The first conclusion of the analysis of the results of these two experiments is that the *Cave* configuration provides worse performance than the *Ninety* configuration for the considered range of α_s in the analysis, because the area $A_{n,max}$ of the *Ninety* configuration is 37% greater than the area $A_{n,max}$ of *Cave* configuration. The second conclusion is that the best performance is provided by the *Ninety* configuration and the *Flower* configuration when $\alpha_s < 65°$ and $\alpha_s > 65°$, respectively. The third conclusion is that the trends of the temperature versus the solar altitude angle for the *Ninety* and *Cave* configurations are similar, but the trend of Flower configuration has a different trend, i.e., the achieved temperature increases monotonically with the solar altitude angle. The maximum temperature of *Flower* configuration is expected to be obtained when the sun is at the zenith. From the plots of Fig. 6, the maximum temperature achieved with *Ninety* and *Cave* configurations is observed when solar altitude angle is around 40°. Thus, it would be useful for the user that the Copenhagen cooker was equipped an extra simple device for determining the solar altitude angle. Manufacturer should also provide information in the user manual of the cooker regarding what configuration should be adopted according to the operation range of the solar altitude angle.

4.2. Analysis of solar cooker performance with high water mass load

In this section, the standardised power $\dot{Q}_S$ is analysed for cooker operation with 1.5 kg of water. From Table 2, the load ratio values of *Cave*, *Flower* and *Ninety* configurations are greater, little greater and little smaller, respectively, than the load ratio recommended by the standard. The experiments with the different cooker configurations were performed in a wide range of average solar altitude angle, i.e., $\bar{\alpha}_s$ between 51° and 72°, that, in average, corresponds to medium and high ranges of values of solar altitude angle.

Figs. 7 and 8 depicts the plots of $\dot{Q}_S$ for the different cooker configurations, respectively, for the medium range and high range of $\bar{\alpha}_s$.

From observation of the results plotted in Fig. 7, it is confirmed that the *Cave* configuration provides power values smaller than the ones

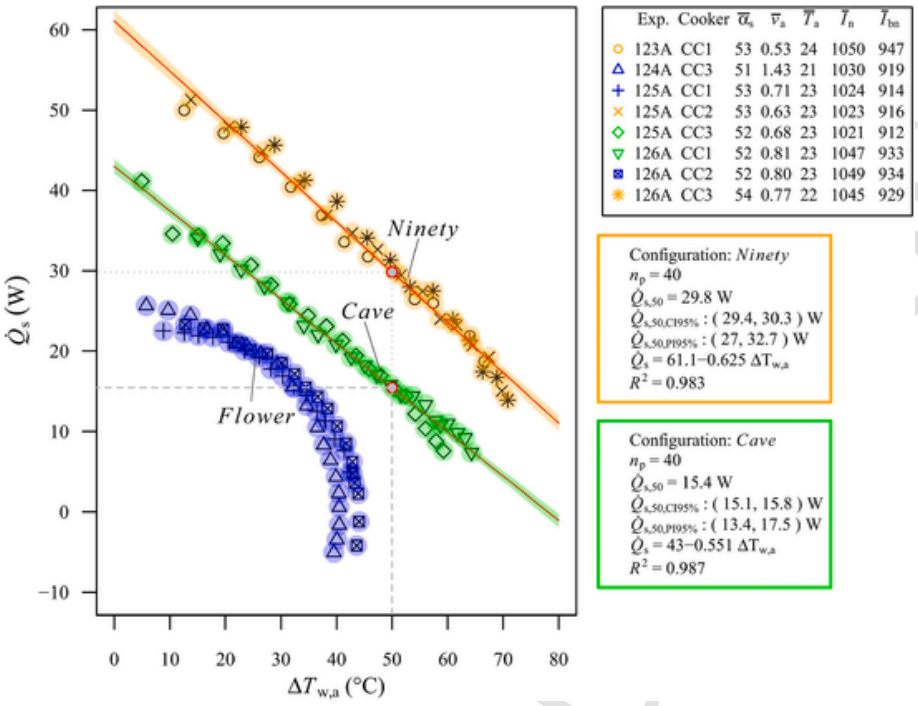

Fig. 7. Plots of $\dot{Q}_S$ as a function of $\Delta T_{w,a}$ at medium solar altitude angles.

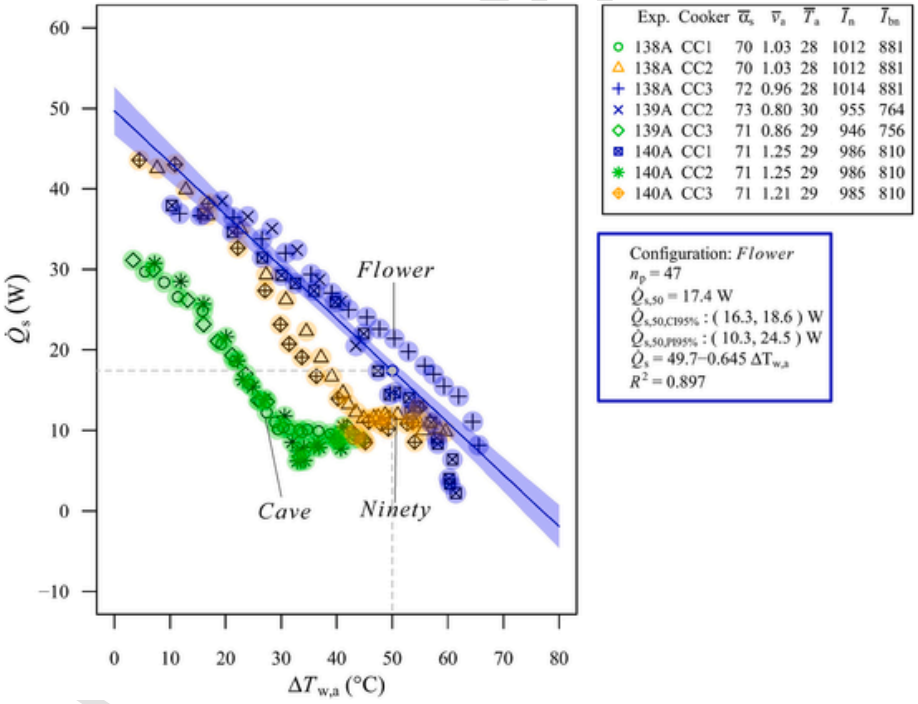

Fig. 8. Plots of $\dot{Q}_S$ as a function of $\Delta T_{w,a}$ at high solar altitude angles.

provided by *Ninety* configuration. From the same figure, the trend of the *Flower* configuration is not linear, the power values are relatively low and the power degradation is more intense in the right half part of the plot. This degradation is due to the increase of thermal losses and to the reduction of cooker performance when solar altitude angle becomes smaller, as depicted in Fig. 6. Regarding the *Cave* and *Ninety* configurations, both plots exhibit a linear trend because each test was conducted with solar altitude angle ranging from 45° to 55°, a range where the variation of performance of the solar cooker without water depicted in Fig. 6 is small. Thus, only the linear regression data recommended by the standard are indicated in Fig. 7 for *Cave* and *Ninety* configurations.

Regarding the experimental results of testing the different cooker configurations depicted in Fig. 8 with sun high elevations, the values of standardised power provided by *Ninety* configuration are higher than the *Flower* configuration in a small range of $\Delta T_{w,a}$ values at the beginning of the load heating process. It is also observed that the values of standardised power provided by *Flower* configuration are higher than the *Ninety* configuration in a relatively large range of $\Delta T_{w,a}$ values,

mainly in middle period of the load heating process. These two opposite behaviours are due to the fact α_s was below 65° at beginning of the test and above 65° in the middle of heating process. From the same Fig. 8, it can be also observed that at the end of the heating process of the load the maximum value of $\Delta T_{w,a}$ in *Ninety* configuration is smaller than the maximum value of $\Delta T_{w,a}$ in *Flower* configuration. Moreover, as shown in Figs. 6–8, it is confirmed that the performance of *Cave* configuration is worse than the performance of the *Ninety* configuration. Therefore, only results of *Ninety* and *Flower* configurations in following studies are analysed.

Another particular aspect to point out is related with the trends of the plots of the *Ninety* and *Cave* configurations depicted in Fig. 8. These two plots do not have a linear trend in all range of $\Delta T_{w,a}$. They have two distinct parts. In the first one, both plots have a large slope due to the heat losses and to the fact that the performance of the cooker decreases when α_s increases as depicted in Fig. 6. In the second part, even the thermal losses are bigger than in first part, the slope is very small because the performance indicator of the cooker represented in Fig. 6 improves with the decreasing of angle α_s. In this second part, these opposite impacts on the power of the cooker are balanced and, for that reason, the changes in power are small.

The performance of the Copenhagen cookers, devices that are designed for operation with only azimuthal adjustments, is influenced significantly by the variations on the angle α_s.

For this reason, the influence of sun elevation on the performance of both *Ninety* and *Flower* is presented in detail in Figs. 9 and 10, where the marks of the points are coloured, being the colour associated with α_s value of the respective time interval.

Fig. 9 encompasses results of 10 tests performed with cooker configuration *Ninety*. There are two different groups of observation points. The first group resulted from a set of 5 tests with an average angle $\bar{\alpha}_s$ between 52° and 54°, being the points represented by yellow or light green marks. The variation of angle α_s in this group of tests corresponds to the range values providing high performance indicator represented in Fig. 6 for the *Ninety* configuration. In the same Fig. 6, the performance indicator is almost constant in all range of angle α_s. For this reason, the plots of Fig. 9 present a linear trend, evidencing that the linear regression can be derived and used. The second group corresponds also to 5 tests that were performed at $\bar{\alpha}_s$ between 64° and 71°. According to the adopted colours for marks of the points in Fig. 9, most of the points, excepting points of the tests 128A-CC2 and 130A-CC1 at end of the process, are outside the range of optimal performance of configuration *Ninety* as shown in Fig. 6 Thus, it explains that the points of the second group of Fig. 9 have lower $\dot{Q}_S$ values than the values of points of the first group.

Regarding the plots of standardised power for the *Flower* configuration in Fig. 10, two groups of points are also identifiable according to the values of angle α_s. The first group of points is made up of three tests with $\bar{\alpha}_s$ ranging from 51° to 53°. As example, in the test 125A-CC1, the α_s values ranged between 46° and 55°. In this range, the performance of the *Flower* configuration is low and it depends strongly on α_s, as shown in Fig. 6, which explains the existence of low $\dot{Q}_S$ values and the curved shape of the plots. The second group of points is made up of 10 tests that were carried out at $\bar{\alpha}_s$ between 65° and 73°. The plots of points in the middle and relatively large range of $\Delta T_{w,a}$ show a linear trend. Contrarily, the plots for the ranges of low and high values of $\Delta T_{w,a}$ present a curved trend. According to the solar altitude angles of these two ranges and to the associated performance indicator shown in Fig. 6, it indicates that cooker in *Flower* configuration was not operating in optimum conditions.

By analysing again Figs. 6, 9 and 10 together, it can be concluded that the use of the *Ninety* and *Flower* configurations are recommendable only when α_s is lower than 65° and greater than 65°, respectively. In addition, changing from one configuration to another is very simple and fast just by changing the right set of snaps. For these reasons, a new configuration, called *NFN* configuration, is considered in a new set of tests carried out with α_s lower and higher than 65°. The test of this new configuration corresponds in fact to make changes of configuration cooker design during the test with the following sequence of configurations: *Ninety*, *Flower* and *Ninety*. The changes are performed when the α_s is approximately 65°.

Fig. 11 depicts the results of the experiment no. 128A, in which three solar cookers were tested side-by-side. Cookers CC1, CC2, CC3 were tested in the *Flower* configuration, the *Ninety* configuration and

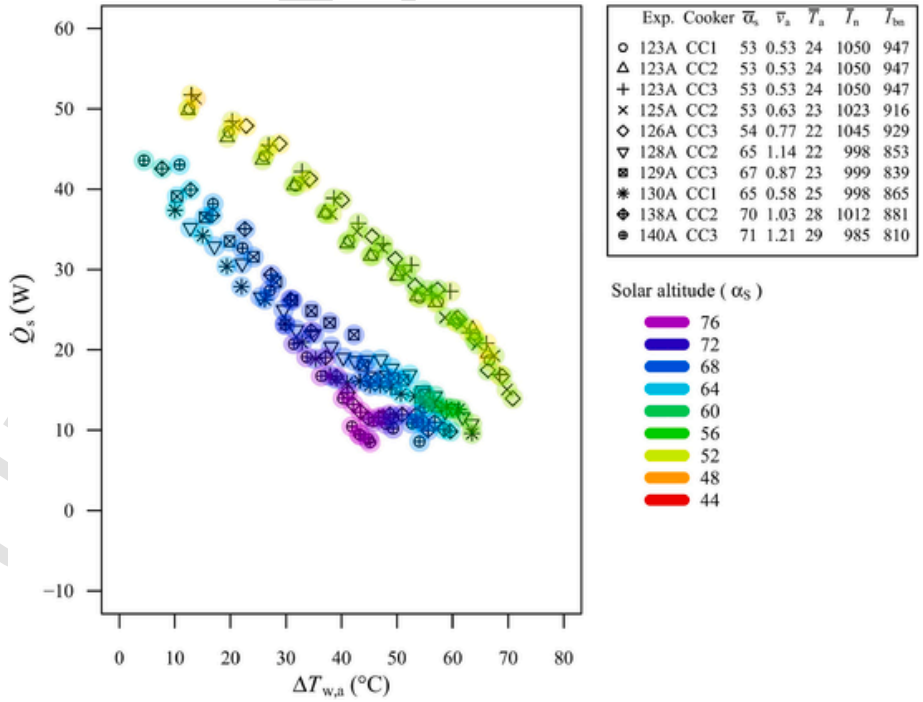

Fig. 9. Plots of $\dot{Q}_S$ versus $\Delta T_{w,a}$ for the *Ninety* configuration.

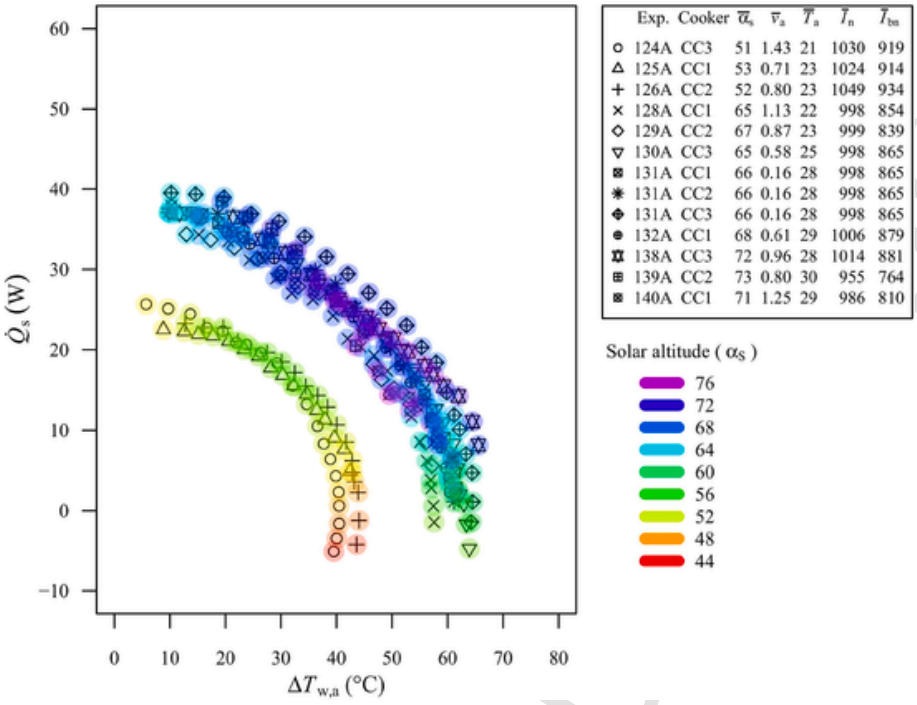

Fig. 10. Plots of $\dot{Q}_S$ versus $\Delta T_{w,a}$ for the *Flower* configuration.

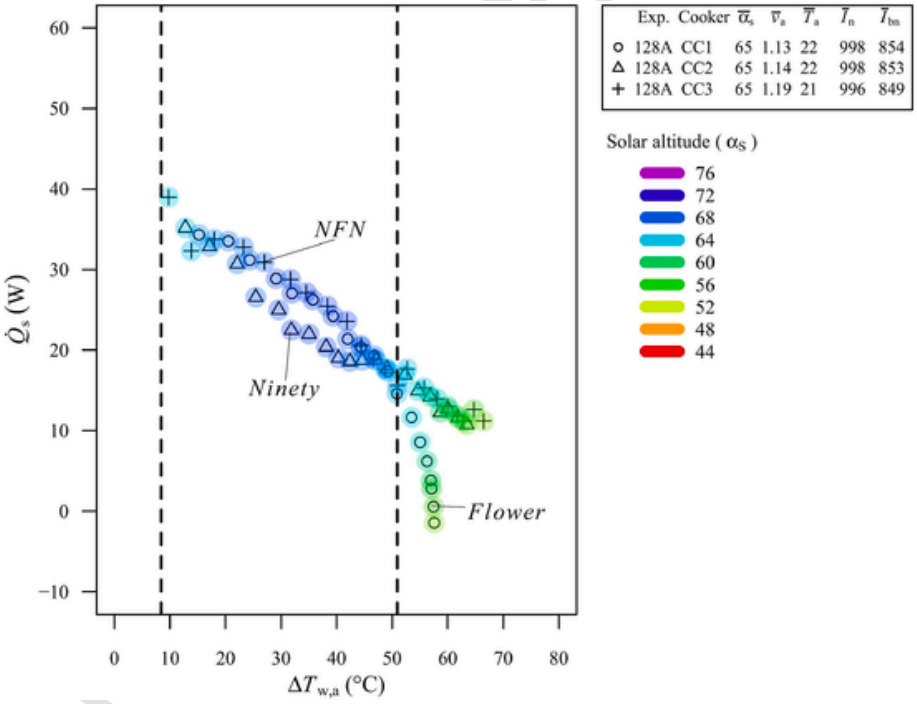

Fig. 11. Plots of $\dot{Q}_S$ versus $\Delta T_{w,a}$ for the *Flower*, *Ninety* and *NFN* configurations.

NFN configuration, respectively. This experiment was carried out when α_s ranged from 54° and 69°. The vertical dashed lines correspond to the instants when configuration of cooker CC3 was changed. None observation points of an initial period of test, i.e., in the let region of the first vertical line, are not plotted because they are not valid observation points. The *Flower* and *NFN* configurations have the same behaviour when α_s is greater than 65°. When α_s is lower than 65°, the *Ninety* and the *NFN* configurations present the same performance. Therefore, the *NFN* configuration provides the best performance, when the minimum and maximum values of α_s are greater and lower than 65°, respectively.

To validate this finding, five tests were performed with the *NFN* configuration. The obtained results are depicted in Fig. 12. It shows that the points obtained for the *NFN* configuration have a linear trend. So, corresponding linear regression data are also indicated in the same Fig. 12.

4.3. Analysis of solar cooker performance with different water loads

The tests considered in previous section *4.2* were done with a water mass of 1.5 kg, which is a relatively high value of the same magnitude given by the load ratio recommended by the standard. In real cooking

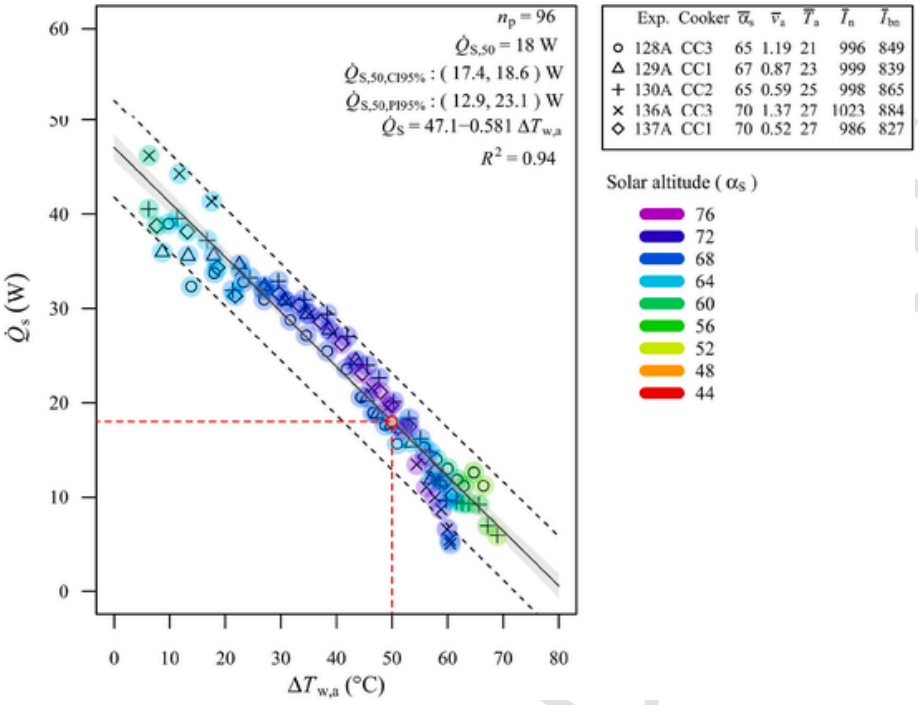

Fig. 12. Plots of $\dot{Q}_S$ versus $\Delta T_{w,a}$ for the *NFN* configuration.

operation with high mass load, 3 to 4 h are needed to load reach the boiling water temperature in the different configurations of the Copenhagen cooker and also in most of panel cookers. If the right configuration is not adopted, the load may not attend the boiling water temperature. Thus, the cooking success result when using a slow cooker depends on the load mass. Therefore, lower mass load values of 1.0 and 0.5 kg are also considered in following studies of present work addressed only with in *NFN* configuration.

Figs. 13 and 14 depict the results of the tests performed with *NFN* configuration for load mass of 0.5 kg and 1.0 kg, respectively by using the same cooking vessel. Figs. 12–14 list the values of the most important parameters of the linear regressions for mass loads of 0.5 kg, 1.0 kg and 1.5 kg.

The use of different load mass values in the same pot causes variation in the volume occupied by the load and its respective level. Consequently, the surface of the pot wall wetted by the load increases with increasing of the load mass. This causes changes in the heat transfer phenomena occurring inside the pot and in the surface of the pot. It is expected that the heating process is more efficient when pot is filled with higher mass of load, but as mentioned before the cooking success result

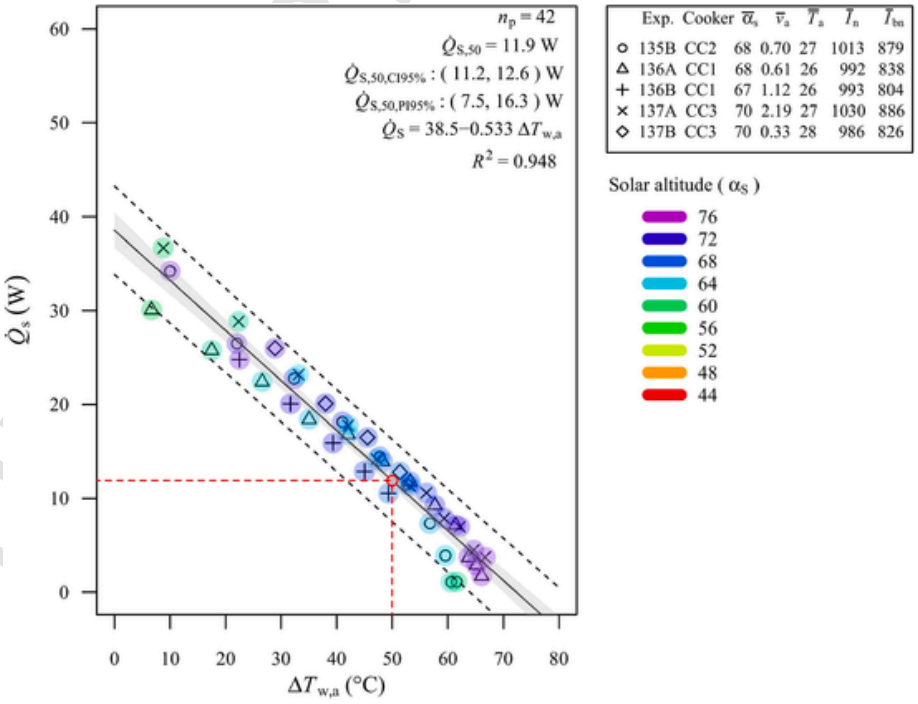

Fig. 13. Plots of $\dot{Q}_S$ versus $\Delta T_{w,a}$ for the *NFN* configuration with load of 0.5 kg.

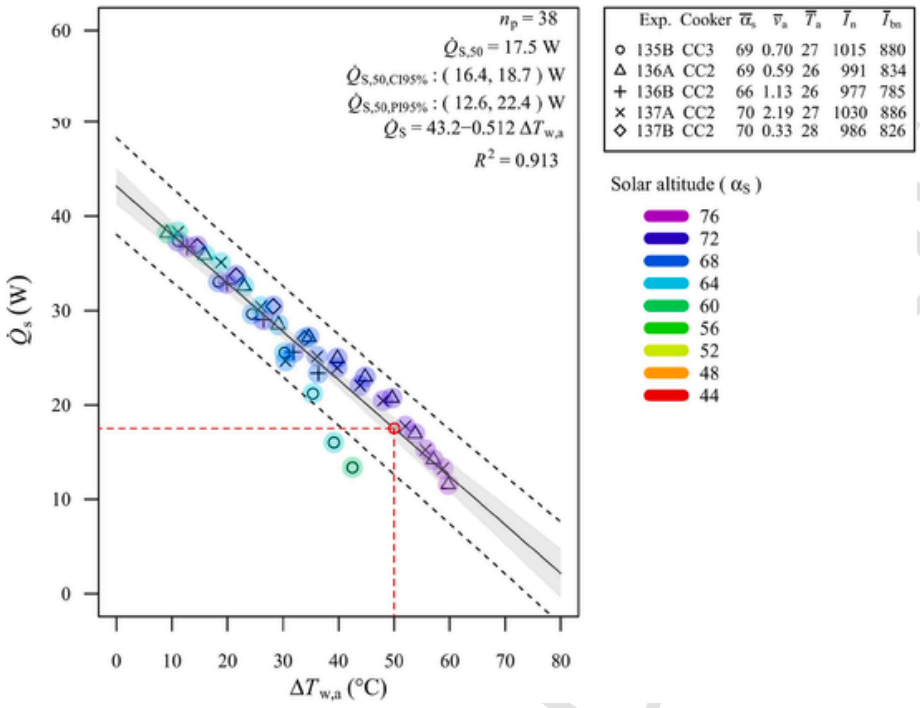

Fig. 14. Plots of $\dot{Q}_S$ versus $\Delta T_{w,a}$ for the *NFN* configuration with load of 1.0 kg.

of a high mass load may not be achieved when cooking period is too long or maximum load temperature is too low.

From Figs. 12–14, the standardised power values of $\dot{Q}_{S,0}$, i.e., standardised power values for $\Delta T_{w,a} = 0$ °C, are 38.5 W, 43.2 W and 47.1 W, respectively, for mass load values of 0.5 kg, 1.0 kg and 1.5 kg. From the same set of figures, the standardised power values of $\dot{Q}_{S,50}$, i.e., standardised power values for $\Delta T_{w,a} = 50$ °C, are 11.9 W, 17.5 W and 18.0 W, respectively, for mass load values of 0.5 kg, 1.0 kg and 1.5 kg. By inspecting the achieved values of $\dot{Q}_{S,0}$ and $\dot{Q}_{S,50}$ for the different mass values of load, it results, as expected, that operation with higher mass load is more efficient than operation with smaller mass load, but for cooking operation of a certain mass of food in common cooking period of around 2 h is better to distribute the amount of food by several cookers. Each cooker would cook a low mass of food.

Even it is difficult to make a comparison of performance of different cooker designs with published data due to several reasons, the performance in terms of standardised power $\dot{Q}_{S,50}$ and the corresponding efficiency η_{50} for the different configurations of Copenhagen solar cooker is compared with performance of other panel cookers. The efficiency η_{50} here introduced is defined by:

$$\eta_{50} = \frac{\dot{Q}_{S,50}}{700\, A_{n,max}} \tag{4}$$

where $A_{n,max}$ is the maximum normal area to the incoming beam irradiation being collected by the solar cooker. The performance data of all panel cookers indicated in Table 1 and the performance data of all configurations of Copenhagen cooker are plotted in Fig. 15. Each point in this figure represents the performance of each cooker design for $\Delta T_{w,a} = 50$ °C or close to this difference value. In case of Copenhagen cooker configurations, the performance data corresponds to tests performed with a load of 1.5 kg. The different cooker designs being analysed in Fig. 15 have different $A_{n,max}$ and were tested with different load ratio values. The best cooker seems to be the Star Flower because it provides biggest values of power and efficiency. The standardised power $\dot{Q}_{S,50}$ for the Copenhagen solar cooker configurations are small

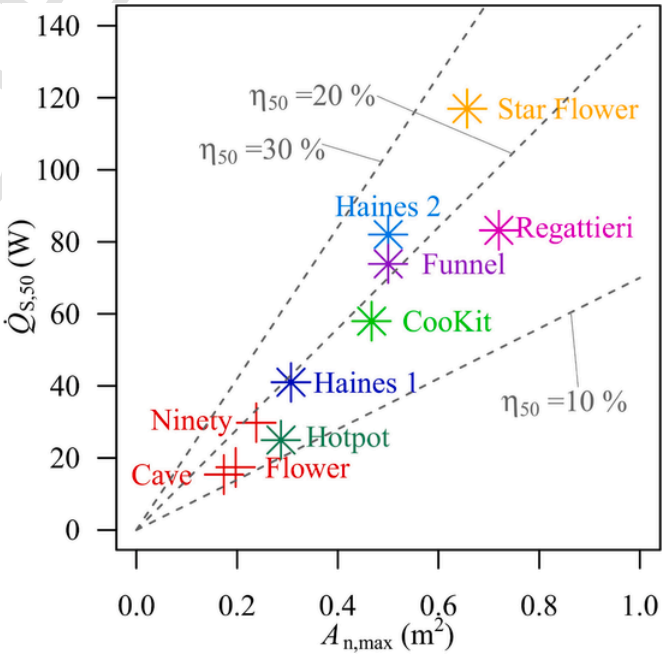

Fig. 15. Performance data of several solar cookers for $\Delta T_{w,a}$ equal or close to 50 °C.

mainly because their $A_{n,max}$ values are small. The performance of the *NFN* configuration has not been represented because its design changing during each test implies changes on the $A_{n,max}$ value. From Fig. 15, it can be observed that the performance of *Ninety* configuration is better than the other two configurations of Copenhagen cooker due to its higher value of $A_{n,max}$. The efficiency η_{50} of *Ninety* configuration is similar to the efficiency of the Haines 1, Funnel and Cookit solar cookers. The *Flower* and *Cave* configurations provide lower values of $\dot{Q}_{S,50}$, due to their smaller values of $A_{n,max}$ and η_{50}. Anyway, because the power values are relatively low, the amount of food that can be cooked in

practice is limited. It is recommended that the design is scaled up to an aperture area of around 0.5 m^2.

5. Conclusions

In present work, three configurations of Copenhagen solar cooker and also a combination of two configurations were tested experimentally, following as closely as possible the ASAE S580.1 [12] standard. Tests were performed in a wide range of solar altitude angles, for three different water mass values.

A particular set of tests without water inside the pot was also performed. The findings obtained from this set of tests, in terms of the dependence of the performance as a function of the solar altitude angle, contribute to a better understanding how in some cases the plot of the standardised power does not evidence a linear trend making impossible the application of the ASAE S580.1 standard in such cases. So, it can be inferred that the procedure supporting the standard is suitable only when the solar altitude angle during a test with an empty cooking vessel does not cause important changes in the solar cooker performance. For this reason, when evaluating the performance of a solar cooker taking into account the ASAE S580.1 standard, it is highly recommended to perform an extra test of cooker with an empty cooking vessel in order to consider valid or not the evaluation obtained by the standard protocol.

From the analysis of the testing results associated with the three main configurations of the Copenhagen cooker, the following findings were achieved. Firstly, in the entire range of solar altitude angle investigated, the *Cave* configuration provides less standardised power values than the *Ninety* configuration. So, the *Cave* configuration recommended by the manufacturer may be discarded from the user manual. Secondly, the *Ninety* and *Flower* configurations provide the best performance when solar altitude angle is below or above 65°, respectively. Thirdly, for tests carried out with a solar altitude angle ranging from a value below 65° to a value above 65°, the best option is to make the following sequential configuration change during the test: *Ninety*, *Flower* and *Ninety*. Fourthly and lastly, the values of maximum aperture area, efficiency and power of the *Ninety* configuration are higher than the *Flower* configuration.

The results obtained from the tests with different amounts of water corroborated what was expected. The performance of the cooker in terms of the reference standardised power value increases with increasing of the mass of the load when using the same pot. The use of amounts of load lower different than the recommended value of the standard, when testing a cooker, is crucial to evaluate the success of real cooking food.

The power of a particular design of cooker is strongly dependent on the its maximum aperture area. In case of the best Copenhagen cooker configuration, the maximum aperture area can range from 0.238 m^2 in *Ninety* to 0.4 m^2 in a new configuration to be investigated in a further research work.

CRediT authorship contribution statement

Xabier Apaolaza-Pagoaga: Supervision, Conceptualization, Methodology, Formal analysis, Investigation, Data curation, Visualization, Writing – original draft, preparation, Writing – review & editingWriting-reviewing & editing. **Antonio Carrillo-Andrés:** Conceptualization, Methodology, Formal analysis, Software, Data curation, Visualization, Writing – review & editingWriting-reviewing & editing. **Celestino Rodrigues Ruivo:** Conceptualization, Methodology, Formal analysis, Writing – review & editingWriting-reviewing & editing.

Declaration of competing interest

The authors declare that they have no known competing financial interests or personal relationships that could have appeared to influence the work reported in this paper.

Acknowledgments

The authors would like to acknowledge Mrs. Sharon Clausson for providing the reflectors of Copenhagen solar cookers.

Appendix A. Data of all tests conducted in the present study

The data associated with all performed experiments with the different version of the Copenhagen solar cooker by using water as load inside the cooking vessel are listed in Table A. The time values correspond to solar time. In some tests, the linear regression data are not reported because the standard protocol [12] is not applicable.

Table A
Data of experiments conducted in Copenhagen solar cookers with water.

Expt. no.	123A	123A	123A	124A	125A	125A	125A	126A
Cooker	CC1	CC2	CC3	CC3	CC1	CC2	CC3	CC1
Configuration	Ninety	Ninety	Ninety	Flower	Flower	Ninety	Cave	Cave
Start time	10:44	10:44	10:44	10:25	10:05	10:05	10:05	10:05
End time	14:00	14:00	14:00	14:00	13:25	13:25	13:25	14:05
Date	22 Mar 2021	22 Mar 2021	22 Mar 2021	23 Mar 2021	24 Mar 2021	24 Mar 2021	24 Mar 2021	25 Mar 2021
m_w (kg)	1.5	1.5	1.5	1.5	1.5	1.5	1.5	1.5
n_p	13	13	13	20	16	14	19	21
$\bar{I}_n$ (W m^{-2})	1050	1050	1050	1030	1024	1023	1021	1047
$\bar{I}_{bn}$ (W m^{-2})	947	947	947	919	914	916	912	933
$\bar{\alpha}_s$ (°)	53	53	53	51	53	53	52	52
$\bar{T}_a$ (°C)	24	24	24	21	23	23	23	23
$\bar{v}_a$ (m s^{-1})	0.53	0.53	0.53	1.43	0.71	0.63	0.68	0.81
$\dot{Q}_{S,50}$ (W)	29.5	29.3	30.9	–	–	29.9	15.0	15.7
$\dot{Q}_{S,0}$ (W)	58.2	57.3	61.4	–	–	61.2	43.9	41.9
a (–)	−0.58	−0.56	−0.61	–	–	−0.63	−0.58	−0.52
R^2	0.995	0.996	0.986	–	–	0.993	0.984	0.997

Expt. no.	126A	126A	128A	128A	128A	129A	129A	129A
Cooker	CC2	CC3	CC1	CC2	CC3	CC1	CC2	CC3
Configuration	Flower	Ninety	Flower	Ninety	9F9	9F9	Flower	Ninety
Start time	10:05	10:05	10:35	10:35	10:35	10:35	10:35	10:35
End time	14:05	14:05	14:00	14:00	14:00	13:35	13:35	13:35
Date	25 Mar 2021	25 Mar 2021	04 May 2021	04 May 2021	04 May 2021	05 May 2021	05 May 2021	05 May 2021
m_w (kg)	1.5	1.5	1.5	1.5	1.5	1.5	1.5	1.5
n_p	19	13	19	20	21	16	16	16
$\overline{I}_n$ (W m^{-2})	1049	1045	998	998	996	999	999	999
$\overline{I}_{bn}$ (W m^{-2})	934	929	854	853	849	839	839	839
$\overline{\alpha}_s$ (°)	52	54	65	65	65	67	67	67
$\overline{T}_a$ (°C)	23	22	22	22	21	23	23	23
$\overline{v}_a$ (m s^{-1})	0.8	0.77	1.13	1.14	1.19	0.87	0.87	0.87
$\dot{Q}_{S,50}$ (W)	–	30.5	–	16.6	18.3	18.4	–	16.2
$\dot{Q}_{S,0}$ (W)	–	65.8	–	39.0	43.0	45.0	–	44.8
a (–)	–	−0.71	–	−0.45	−0.49	−0.53	–	−0.57
R^2	–	0.988	–	0.969	0.975	0.934	–	0.986

Expt. no.	130A	130A	130A	131A	131A	131A	132A	135B
Cooker	CC1	CC2	CC3	CC1	CC2	CC3	CC1	CC2
Configuration	Ninety	9F9	Flower	Flower	Flower	Flower	Flower	9F9
Start time	10:15	10:15	10:15	10:15	10:15	10:15	10:15	12:15
End time	14:00	14:00	14:00	13:55	13:55	13:55	13:56	13:55
Date	06 May 2021	06 May 2021	06 May 2021	07 May 2021	07 May 2021	07 May 2021	13 May 2021	21 May 2021
m_w (kg)	1.5	1.5	1.5	1.5	1.5	1.5	1.5	0.5
n_p	22	23	22	19	20	20	20	10
$\overline{I}_n$ (W m^{-2})	998	998	998	998	998	998	1006	993
$\overline{I}_{bn}$ (W m^{-2})	865	865	865	865	865	865	879	804
$\overline{\alpha}_s$ (°)	65	65	65	66	66	66	68	67
$\overline{T}_a$ (°C)	25	25	25	28	28	28	29	26
$\overline{v}_a$ (m s^{-1})	0.58	0.59	0.58	0.16	0.16	0.16	0.61	1.12
$\dot{Q}_{S,50}$ (W)	14.7	18.5	–	–	–	–	–	10.6
$\dot{Q}_{S,0}$ (W)	38.2	47.8	–	–	–	–	–	41.7
a (–)	−0.47	−0.59	–	–	–	–	–	−0.62
R^2	0.916	0.957	–	–	–	–	–	0.968

Expt. no.	135B	136A	136A	136A	136B	136B	137A	137A
Cooker	CC3	CC1	CC2	CC3	CC1	CC2	CC1	CC2
Configuration	9F9	9F9	9F9	9F9	9F9	9F9	9F9	9F9
Start time	12:35	9:55	9:55	9:55	12:15	12:15	9:55	9:55
End time	13:55	11:55	11:55	13:15	13:15	13:15	13:15	11:55
Date	21 May 2021	24 May 2021	24 May 2021	24 May 2021	24 May 2021	24 May 2021	25 May 2021	25 May 2021
m_w (kg)	1.0	0.5	1.0	1.5	0.5	1.0	1.5	1.0
n_p	7	12	11	19	5	5	17	11
$\overline{I}_n$ (W m^{-2})	977	1013	1015	1023	1030	1030	986	991
$\overline{I}_{bn}$ (W m^{-2})	785	879	880	884	886	886	827	834
$\overline{\alpha}_s$ (°)	66	68	69	70	70	70	70	69
$\overline{T}_a$ (°C)	26	27	27	27	27	27	27	26
$\overline{v}_a$ (m s^{-1})	1.13	0.7	0.7	1.37	2.19	2.19	0.52	0.59
$\dot{Q}_{S,50}$ (W)	8.9	11.5	18.8	16.2	10.2	15.4	18.7	18.3
$\dot{Q}_{S,0}$ (W)	47.2	34.5	44.0	53.5	36.8	44.2	45.7	43.5
a (–)	−0.77	−0.46	−0.50	−0.74	−0.53	−0.58	−0.54	−0.50
R^2	0.979	0.975	0.979	0.973	0.999	0.999	0.953	0.974

Expt. no.	137A	137B	137B	138A	138A	138A	139A	139A
Cooker	CC3	CC2	CC3	CC1	CC2	CC3	CC2	CC3
Configuration	9F9	9F9	9F9	Cave	Ninety	Flower	Flower	Cave
Start time	9:55	12:15	12:15	9:55	9:55	9:55	10:02	10:02
End time	11:55	13:15	13:15	13:55	13:55	13:55	13:54	13:54
Date	25 May 2021	25 May 2021	25 May 2021	07 Jun 2021	07 Jun 2021	07 Jun 2021	09 Jun 2021	09 Jun 2021
m_w (kg)	0.5	1.0	0.5	1.5	1.5	1.5	1.5	1.5
n_p	11	4	4	23	23	18	7	9
$\overline{I}_n$ (W m^{-2})	992	986	986	1012	1012	1014	955	946
$\overline{I}_{bn}$ (W m^{-2})	838	826	826	881	881	881	764	756
$\overline{\alpha}_s$ (°)	68	70	70	71	71	72	73	71
$\overline{T}_a$ (°C)	26	28	28	28	28	28	30	29
$\overline{v}_a$ (m s^{-1})	0.61	0.33	0.33	1.0	1.03	0.96	0.80	0.86
$\dot{Q}_{S,50}$ (W)	13.3	19.3	13.6	–	–	20.4	18.7	–
$\dot{Q}_{S,0}$ (W)	44.6	44.3	42.5	–	–	46.7	53.6	–
a (–)	−0.57	−0.50	−0.58	–	–	−0.52	−0.70	–

Expt. no.	137A	137B	137B	138A	138A	138A	139A	139A
R^2	0.998	0.995	0.997	–	–	0.965	0.932	–

Expt. no.	140A	140A	140A
Cooker	CC1	CC2	CC3
Configuration	Flower	Cave	Ninety
Start time	9:54	9:54	9:54
End time	13:54	13:54	13:54
Date	10 Jun 2021	10 Jun 2021	10 Jun 2021
$m_w\,(kg)$	1.5	1.5	1.5
n_p	22	22	23
$\bar{I}_n\,(\mathrm{W\,m^{-2}})$	986	986	986
$\bar{I}_{bn}\,(\mathrm{W\,m^{-2}})$	810	810	810
$\bar{\alpha}_s\,(^o)$	71	71	71
$\bar{T}_a\,(^o\mathrm{C})$	29	29	29
$\bar{v}_a\,(\mathrm{m\,s^{-1}})$	1.25	1.25	1.21
$\dot{Q}_{S,50}$ (W)	14.6	–	–
$\dot{Q}_{S,0}$ (W)	49.9	–	–
$a\,(-)$	−0.71	–	–
R^2	0.956	–	–

References

[1] M. Aramesh, M. Ghalebani, A. Kasaeian, H. Zamani, G. Lorenzini, O. Mahian, S. Wongwises, A review of recent advances in solar cooking technology, Renew. Energy 140 (2019) 419–435, https://doi.org/10.1016/j.renene.2019.03.021.

[2] N.L. Panwar, S.C. Kaushik, Surendra Kothari, State of the art of solar cooking: an overview, Renew. Sustain. Energy Rev. 16 (2012) 3776–3785, https://doi.org/10.1016/j.rser.2012.03.026.

[3] E. Cuce, P.M. Cuce, A comprehensive review on solar cookers, Appl. Energy 102 (2013) 1399–1421, https://doi.org/10.1016/j.apenergy.2012.09.002.

[4] Solar Cookers International. Solar cooker designs. https://solarcooking.fandom.com/wiki/Category:Solar_cooker_designs (Accessed 13 May 2021).

[5] Solar Cookers International. Refugee camps. https://solarcooking.fandom.com/wiki/Refugee_camps (Accessed 13 May 2021).

[6] M. Owen, Cooking Options in Refugee Situations. A Handbook of Experiences in Energy Conservation and Alternatives Fuels, Environment Unit, Engineering and Environmental Services Section, UNHCR, 2002.

[7] J. Barbieri, F. Riva, E. Colombo, Cooking in refugee camps and informal settlements: a review of available technologies and impacts on the socio-economic and environmental perspective, Sustain. Energy Technol. Assess. 22 (2017) 194–207, https://doi.org/10.1016/j.seta.2017.02.007.

[8] Test Results, Solar Cookers International. https://www.solarcookers.org/work/research/results (Accessed 28 May 2021).

[9] C. Ruivo, A. Carrillo-Andrés, X. Apaolaza-Pagoaga, Experimental determination of the standardised power of a solar funnel cooker for low sun elevations, Renew. Energy 170 (2021) 364–374, https://doi.org/10.1016/j.renene.2021.01.146.

[10] S.L. Clausson, A comparison of Copenhagen solar cookers with other similar sized solar cookers, in: CONSOLFOOD 2018, Faro, Portugal, 2018, 22–24 January.

[11] Copenhagen Solar Cooker Light, Solar cooking Wiki. https://solarcooking.fandom.com/wiki/Copenhagen_Solar_Cooker_Light (Accessed 13 May 2021).

[12] ASAE S580.1 NOV2013, Testing and Reporting Solar Cooker Performance, American Society of Agricultural Engineers, Michigan, USA, 2013.

[13] E. Pejack, Optical properties of the Cookit solar cooker, in: Proceedings of the 2006 Solar Cookers International Conference, 2006, Granada, España. http://solarcooking.org/Granada06/133_ed_pejack.pdf.

[14] S.M. Ebersviller, J.J. Jetter, Evaluation of performance of household solar cookers, Sol. Energy 208 (2020) 166–172, https://doi.org/10.1016/j.solener.

[15] A. Regattieri, F. Piana, M. Bortolini, M. Gamberi, E. Ferrari, Innovative portable solar cooker using the packaging waste of humanitarian supplies, Renew. Sustain. Energy Rev. 57 (2016) 319–326, https://doi.org/10.1016/j.rser.2015.12.199.

[16] P. Arveson, Procedure for Determining the Intercept Area of a Solar Cooker, Technical Report no. TR-10. Solar Household Energy, Inc., 2017.

[17] J.A. Duffie, W.A. Beckman, Solar Engineering of Thermal Processes, fourth ed., Willey, 2013.